

# A Unique G-Quadruplex Aptamer: A Novel Approach for Cancer Cell Recognition, Cell Membrane Visualization, and RSV Infection Detection

Chao-Da Xiao <sup>1,2,\*,†</sup>, Ming-Qing Zhong <sup>1,2,†</sup>, Yue Gao <sup>1</sup>, Zheng-Lin Yang <sup>1</sup>, Meng-Hao Jia <sup>1</sup>, Xiao-Hui Hu <sup>1</sup>, Yan Xu <sup>3</sup> and Xiang-Chun Shen <sup>1,2,\*</sup>

<sup>1</sup> State Key Laboratory of Functions and Applications of Medicinal Plants, School of Pharmaceutical Sciences, Guizhou Medical University, Guiyang 550025, China; zhongmingqing163@163.com (M.-Q.Z.); gaoyue2308@163.com (Y.G.); crazyyang168@163.com (Z.-L.Y.); jiamenghao0522@163.com (M.-H.J.); 19985602747@163.com (X.-H.H.)

<sup>2</sup> The Key Laboratory of Optimal Utilization of Natural Medicine Resources, School of Pharmaceutical Sciences, Guizhou Medical University, Guiyang 550025, China

<sup>3</sup> Division of Chemistry, Department of Medical Sciences, Faculty of Medicine, University of Miyazaki, Miyazaki 889-1692, Japan; xuyan@med.miyazaki-u.ac.jp

\* Correspondence: xcd@gmc.edu.cn (C.-D.X.); sxc@gmc.edu.cn (X.-C.S.)

† These authors contributed equally to this work.

**Mutant sequence: GUUAGAGUUUAUGAGAUUG**

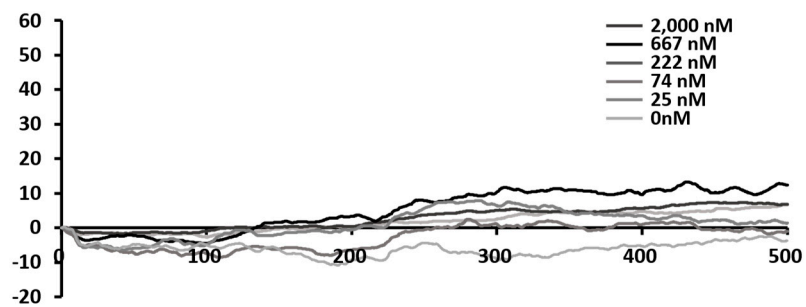
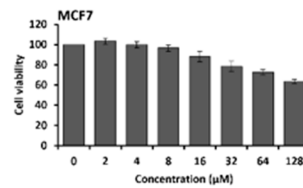
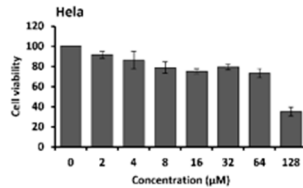
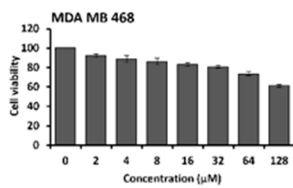


**Figure S1.** Sensorgrams showing mutant sequence - NCL binding (resonance units vs. time) with increasing aptamer concentration from 0  $\mu$ M to 2  $\mu$ M.

**Apt-3 MTT**



**AS1411 MTT**

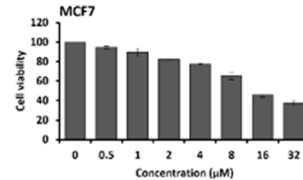
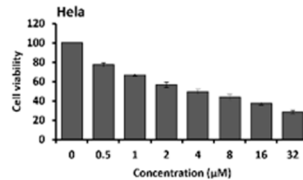
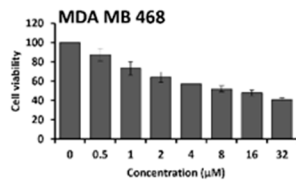


**Figure S2.** The cytotoxicity of Apt 3 and AS1411 was evaluated in MDA MB 468, HeLa, and MCF 7 cells through an MTT assay.

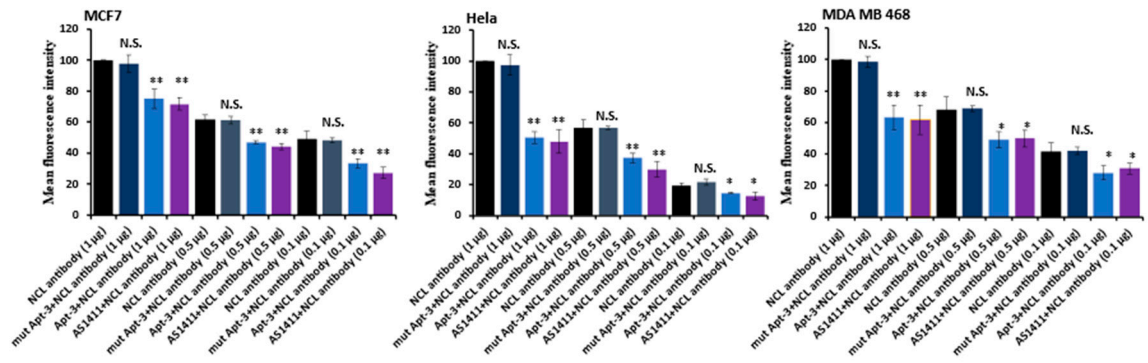


**Figure S3.** IHC + flow cytometry confirmed Apt-3 binding to NCL on cell membranes of MCF-7 **a**, Hela **b**, MDA MB 468 **c**. Data were expressed as the mean  $\pm$  SEM ( $n=3$ ). \*\* $p < 0.01$ . \* $p < 0.05$ . (Student's  $t$  test).

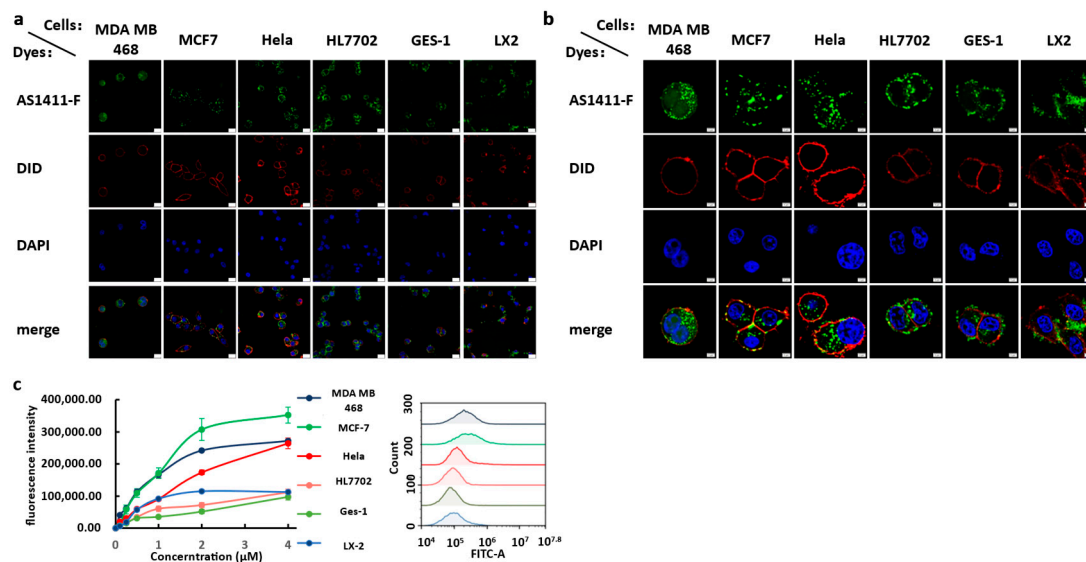


**Figure S4. a** Laser confocal microscope images of cancer and normal cells treated with 2  $\mu$ M AS1411-F. Scale bar is 20  $\mu$ m. Green channel:  $\lambda_{ex}=488$  nm,  $\lambda_{em}=500-530$  nm, blue channel:  $\lambda_{ex}=405$  nm,  $\lambda_{em}=440-470$  nm, red channel:  $\lambda_{ex}=561$  nm,  $\lambda_{em}=600-700$  nm. **b** High magnification images displaying the cell membrane staining of AS1411-F. Scale bar is 5  $\mu$ m. **c** Left side: mean fluorescence intensity variations of different cell staining with increasing concentrations of AS1411-F detected by a flow cytometer with a fixed wavelength at  $\lambda_{ex}=488$  nm,  $\lambda_{em}=530$  nm. right side: The flow cytometry representation results for various cells at a 1  $\mu$ M concentration of AS1411-F.

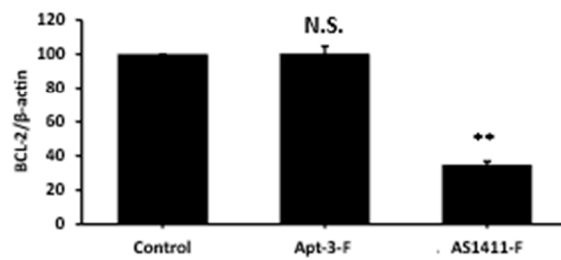
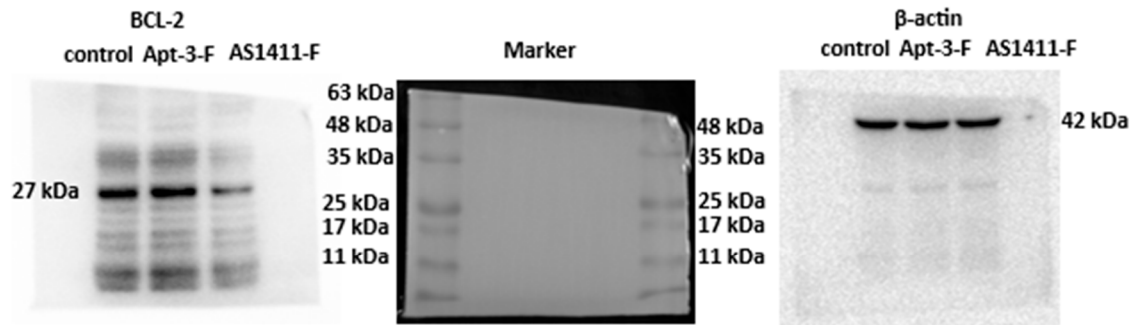


**Figure S5.** Western blot analysis of BCL-2 protein expression in HeLa cells treated with Apt-3-F (10  $\mu$ M) or AS1411 (10  $\mu$ M). Data were expressed as the mean  $\pm$  SEM ( $n=3$ ). \*\* $p < 0.01$  (Student's  $t$  test). N.S. (nonsignificant) =  $p > 0.05$ , vs. Ctrl group.

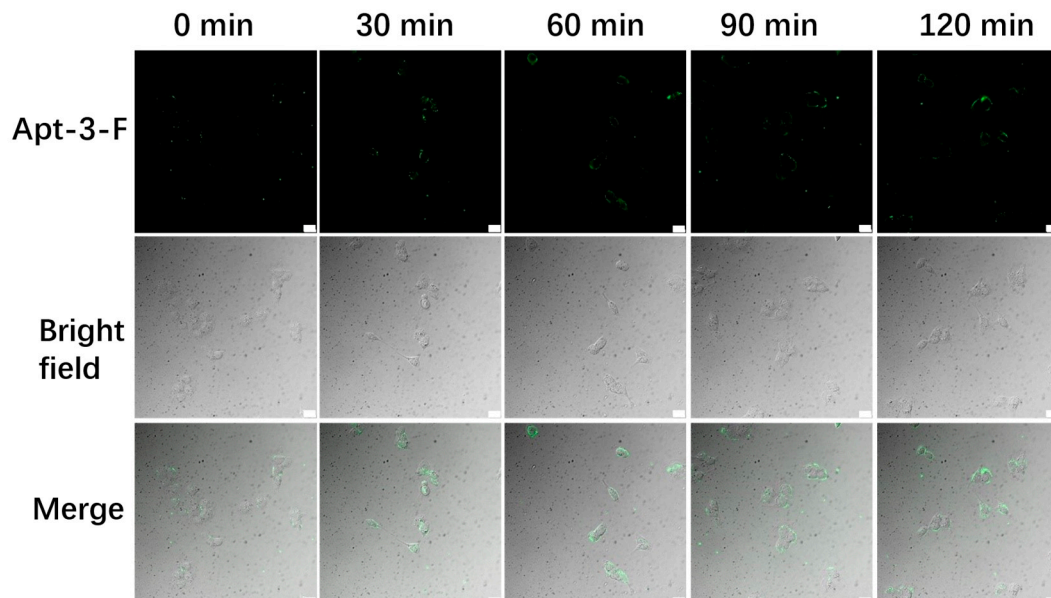


**Figure S6.** Apt-3-F staining images of MDCK cells treated with RSV for different time. Scale bar: 20  $\mu$ m

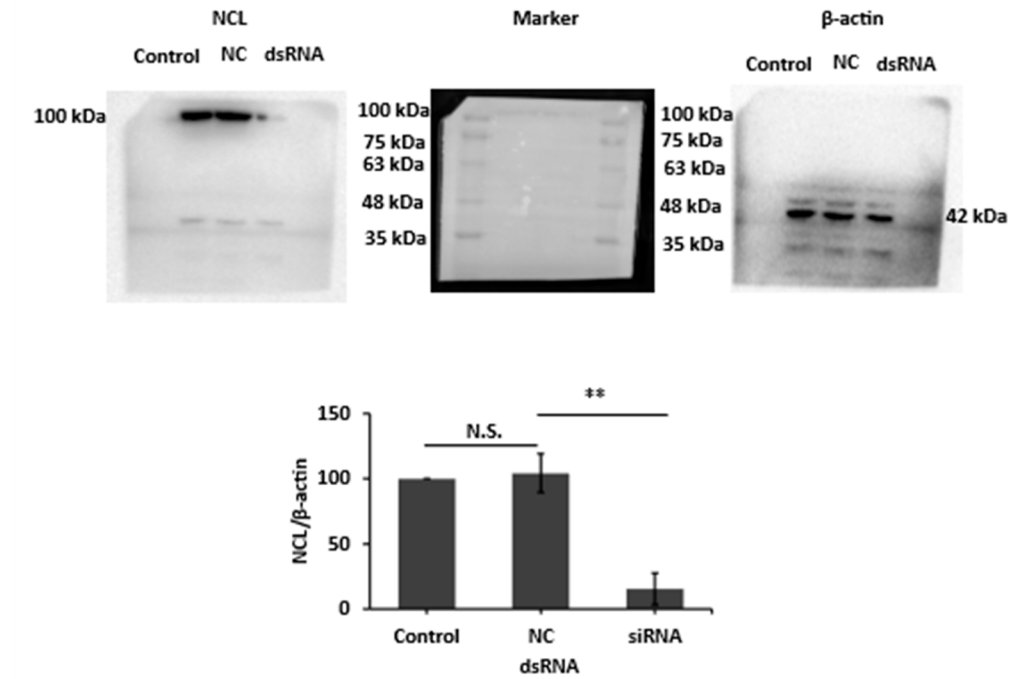


**Figure S7.** NCL expression was inhibited upon transfection of dsRNA into HeLa cells. The lower histograms depict the percentage of NCL repression achieved through RNAi inhibition. Data were expressed as the mean  $\pm$  SEM ( $n=3$ ). \*\* $p < 0.01$  (Student's  $t$  test).

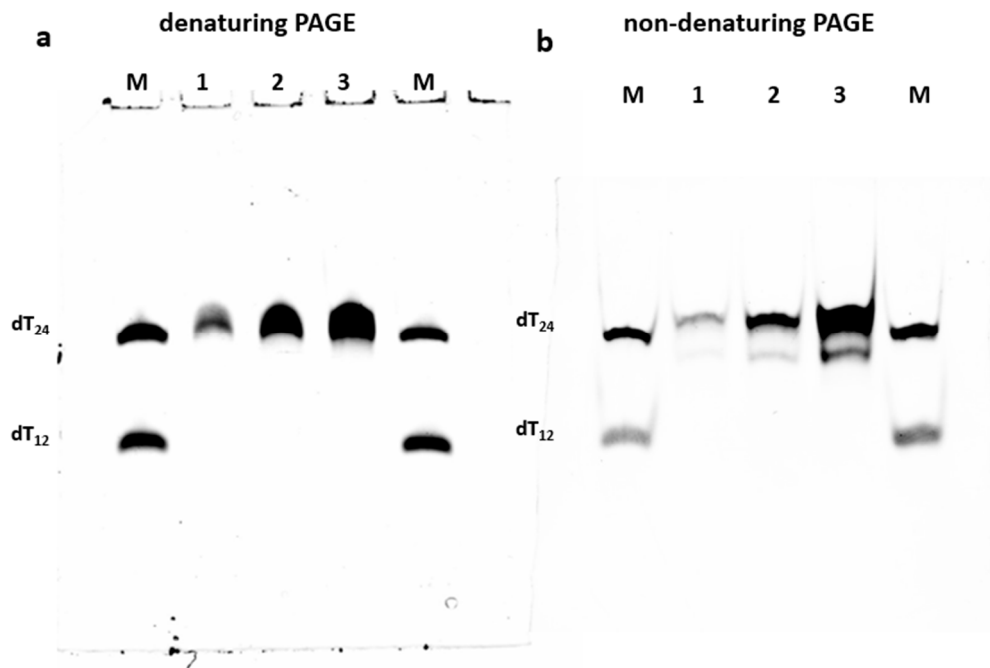


**Figure S8.** Denaturing and non-denaturing PAGE images of Apt-3. Lane M, makers dT<sub>12</sub> and dT<sub>24</sub>; lane 1, 2, and 3, Apt-3 (100, 200 and 400 pmol).